

Effects of Interchannel Coupling in Associative Detachment: Electron Spectra for $\text{H} + \text{Cl}^-$ and $\text{H} + \text{Br}^-$ Collisions

S. Živanov and M. Allan

Department of Chemistry, University of Fribourg, Chemin du Musée 9, 1700 Fribourg, Switzerland

M. Čížek and J. Horáček

Institute of Theoretical Physics, Faculty of Mathematics and Physics, Charles University Prague, V Holešovičkách 2, 180 00 Praha 8, Czech Republic

F. A. U. Thiel and H. Hotop

Department of Physics, University of Kaiserslautern, D-67653 Kaiserslautern, Germany

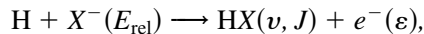
(Received 6 April 2002; published 30 July 2002)

We present experimental and theoretical energy spectra of the electrons detached in collisions of slow Cl^- and Br^- ions with atomic hydrogen. Nonlocal resonance theory predicts two kinds of features in the spectra: steplike structures associated with rovibrational onsets and steep rises associated with interchannel coupling, the latter being absent in a calculation using the simpler local-complex potential theory. Our experimental spectra confirm the presence of both types of structures and thus the necessity of including interchannel coupling to properly describe the product-state distribution.

DOI: 10.1103/PhysRevLett.89.073201

PACS numbers: 34.80.Gs

Introduction.—A recent theoretical treatment [1] of associative electron detachment (AD)



(where E_{rel} is the center-of-mass collision energy and ε the electron energy) concluded that use of the nonlocal resonance theory is essential for $X = \text{F}, \text{Cl},$ and Br , where the departing electron is predominantly s -wave. It leads to a prediction of a distribution of the final states (v, J) differing qualitatively from that of the simpler local-complex-potential (LCP) theory.

The LCP concept has been used successfully in many instances to describe electron-molecule collisions [2], Penning and associative ionization processes [3,4], and the associative electron detachment in $\text{H} + \text{H}^- \ ^2\Sigma_u^+$ collisions [5]. It fails to properly describe threshold effects such as the Wigner cusps in dissociative electron attachment to hydrogen halides [6], however. The more general nonlocal resonance theory [7] overcomes these shortcomings and has been shown to reproduce all observed features in low-energy electron collisions with hydrogen halides [8]. Alternative approaches, which are able to describe threshold features in resonance collisions, are R -matrix theory [9,10] and its limiting case, the zero-range-potential (ZRP) approximation. The latter was used for calculations of F^-/H and Cl^-/H associative detachment by Gauyacq [11].

The dramatic difference between the predictions of the LCP and the nonlocal theories, illustrated in Fig. 1 for the $\text{H} + \text{Br}^-$ system, renders the measurement of the energy spectra a critical experimental test of the theoretical models. The nonlocal theory predicts two kinds of structures [1]. The first kind are steplike structures at the respective

rotational onsets for the formation of the product molecules in the various vibrational states ($v = 0, 1, 2$ for HCl , $v = 0, 1$ for HBr). The second kind of structure is associated with the rotational closing of the highest accessible vibrational channel v_{max} for rotational angular momenta J beyond the maximum value J_m . Because of strong interchannel coupling, not properly accounted for in the LCP theory, steplike onsets (labeled S_v) are observed in the rotational distributions for the lower vibrational levels ($v < v_{\text{max}}$) at $J = J_m$; they are located at the energy $\varepsilon(S_v) = G(v_{\text{max}}) - G(v) + (B_{v_{\text{max}}} - B_v)J_m(J_m + 1)$. Typically, the rotational energy difference is small compared to the vibrational term difference; i.e., the onset energy for the step S_v is simply located at the energy difference

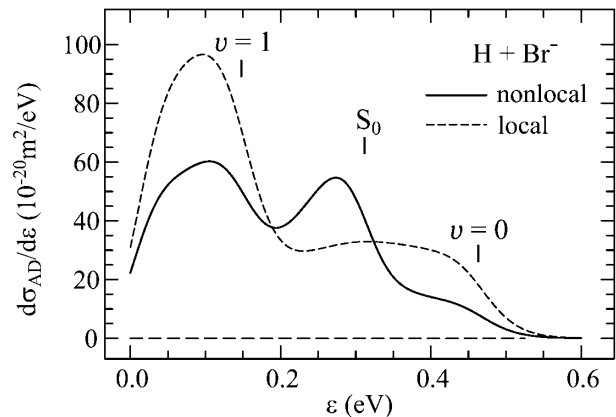


FIG. 1. Energy spectra of electrons detached in $\text{H} + \text{Br}^-$ collisions, calculated within the nonlocal (solid line) and local (dashed line) theories for a mean collision energy of 88 meV and a Gaussian electron resolution function with 60 meV width.

$G(v_{\max}) - G(v)$ which is independent of collision energy. This fact is favorable for the experimental detection of these characteristic structures.

Early experimental studies of associative detachment measured the rate coefficients [12]. Huels *et al.* [13] determined the total cross sections for associative detachment in $H + X^-$ collisions as a function of collision energy in a crossed beam experiment and found them, in agreement with a classical model calculation, to increase rapidly with decreasing collision energy. The total cross sections do not represent a sensitive probe of the theoretical description, however, because they do not provide information on the distribution of the final vibrational and rotational states of the product molecules. The ratio of the (rotationally summed) populations of the $v = 2$ and $v = 1$ final vibrational levels in HCl was determined from infrared chemiluminescence in a flowing afterglow to be 0.60 ± 0.03 [14], in agreement with the results of the ZRP calculation (0.612 [11]) and the nonlocal resonance theory (0.574 [1]), whereas LCP theory (1.32 [1]) is much too high. Similar measurements were performed for the F^-/H and F^-/D systems [15]. This Letter provides detailed information on both the final vibrational and rotational state populations by measuring the energy spectra of the detached electrons.

Methods.—The intricacy of the present experiment stems from the fact that both collision partners have to be prepared *in situ*. The yield of the detached electrons is consequently low and requires high sensitivity of the electron-energy analyzer. Preparing the halogen negative ions with sufficiently low energies and detecting very slow electrons with controlled response function represent additional challenges. The instrumental setup which we constructed for the present experiment is based on the magnetically collimated electron spectrometer described in [16,17] and is shown in Fig. 2. The trochoidal electron-energy analyzer [18] provides the required high sensitivity and low-energy capacity. The possibility to operate the instrument both in the electron-energy loss and the associative detachment modes was useful for optimizing the yield of atomic hydrogen and tuning the electron analyzer.

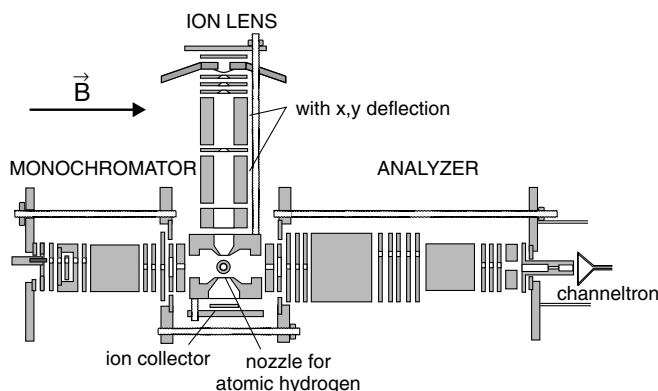


FIG. 2. Schematic diagram of the instrument.

Cl^- or Br^- anions are generated by dissociative electron attachment to hot CCl_4 and CBr_4 , respectively, in the vicinity of a hot filament, in a way similar to that used previously to prepare O^- [19]. The ions are focused into the collision region by a three-cylinder lens designed with the CPO-3D program [20]. The ion lens is immersed in the magnetic field of the trochoidal spectrometer, and this field separates the anions and the electrons emanating from the filament. The fact that ions are never accelerated to more than about 20 eV permits low final ion energies, down to about 0.5 eV.

The nominal lab-frame ion energies are given by the voltage difference between the filament and the collision region. Differences in contact potentials between the filament and the molybdenum parts around the collision region could make the true ion energy different from the nominal energy, but retarding potential analysis indicates that the difference is less than 0.3 eV and we neglected it. The width of the energy distribution of the ions appears to be essentially thermal at the temperature of the filament (below 0.3 eV). This energy spread and energy accuracy are adequate because they are greatly compressed in the center-of-mass frame [1]. Ion currents of typically 200 pA were attained. The collision region consists of two conical electrodes with apertures for the ion beam.

The atomic hydrogen source follows the design of Paolini and Khakoo [21]. It uses a microwave discharge in an air-cooled fused silica tube to dissociate H_2 . The discharged hydrogen passes a 1 mm constriction in the silica tube, is led by a ~ 20 cm long polytetrafluoroethylene tube to a nozzle made of fused silica with a 1 mm diameter exit, painted with graphite on the outside. The hydrogen atoms enter in a direction perpendicular to that of the ion and electron beams. The mixed H, H_2 target was characterized by inelastic electron scattering over the energy loss range 9–13 eV, relevant for excitation of $H^*(n = 2, 3)$ and $H_2^*(B^1\Sigma_u^+, c^3\Pi_u)$. The $H^*(n = 2)$ peak was typically $10\times$ higher than the most intense molecular band (when excited 0.5 eV above threshold). The residual molecular hydrogen does not contribute to the associative detachment signal at the relevant collision energies. Admixture of small amounts of water vapor to the discharge [22] increased the yield of atomic hydrogen two- to threefold. We verified that the water vapor makes no measurable contribution to the associative detachment spectra.

The energy scales cannot be calibrated in the usual way on N_2 , because the discharged hydrogen causes large drifts of the contact potentials of the electrodes and calibration has to be made in the presence of H. We therefore calibrated the onset of the electron signal on the position of narrow resonant structures in the differential cross section for the excitation of the $n = 2$ transitions of atomic hydrogen, which we know from high-level convergent close coupling calculations of Bray [23]. The scale is reliable to ± 30 meV. The resolution of the analyzer is 50–60 meV. The spectra have been corrected for the response function

of the analyzer, based on our previous experiments with helium and on a numerical treatment of electron trajectories [17]. The correction procedure is reliable to within about $\pm 30\%$ at energies above 100 meV, less reliable below. Our experiment measures relative cross sections. We compare the shapes of the experimental and the theoretical curves, but not the absolute magnitudes.

We constructed the nonlocal resonance model for $X = \text{Cl}$ and Br from *ab initio* electron-molecule calculations with fixed geometry of the molecule [1,8,24]. For each system, the model is described by the potential $V_0(R)$ of the neutral molecule, the discrete state potential $V_d(R)$, and the coupling $V_{d\varepsilon}(R)$ of the discrete state and the continuum, which depends on both electron energy ε and internuclear separation R . Employing the nonlocal resonance theory, we calculated the associative detachment cross section $\sigma_{v,J}(E)$ for each rovibrational state of the HX molecule formed. For comparison we also calculated the cross sections with the local-complex potential method. (For the present polar molecules, it is not possible to define the LCP model uniquely from *ab initio* data. We verified that the result shown in Fig. 1 is not sensitive to the details of the parameter choice.) To predict the electron spectrum for the beam experiment, we assumed that the anion beam (with a well-defined energy E_{ion}) collides with a perpendicular beam of hydrogen atoms with a Maxwell-Boltzmann distribution of energies. Associative detachment cross sections are averaged over the center-of-mass collision energy distribution for this experimental setup. In addition, the spectra have been convoluted with a Gaussian of 60 meV width (FWHM) to take into account the resolution of the electron spectrometer.

Results and discussion.—Figure 3 shows the experimental spectrum of electrons detached in $\text{H} + \text{Br}^-$ collisions compared to the theoretical prediction. The rotational onsets are marked by vertical bars and the values of the corresponding ν . The signals to the left of these onsets are due to the formation of increasingly rotationally excited products. The cross section for $\nu = 0$ rises at a given

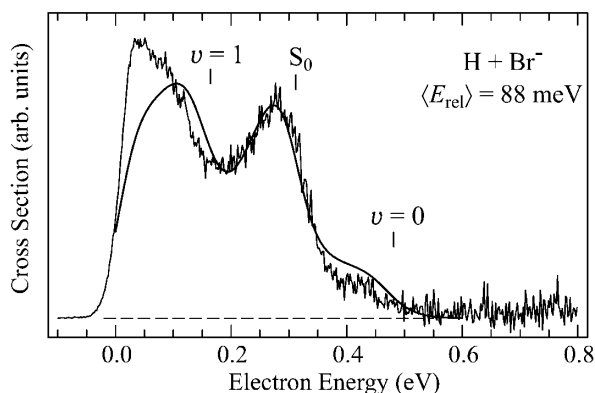


FIG. 3. Experimental and theoretically predicted (smooth line) spectra of electrons detached in $\text{H} + \text{Br}^-$ collisions. The laboratory frame ion energy was 4 eV.

J as a consequence of the closure of the $\nu = 1$ vibrational channel at that J , and the corresponding electron energy is marked S_0 . The experimental curve clearly confirms the presence of *both* types of steps. The theoretical and experimental curves agree well at energies above 100 meV. The experiment indicates a higher yield of electrons below 100 meV, but the difference could be due to the reduced reliability of correcting the experimental spectra for the analyzer response function at very low energies.

The spectrum resulting from $\text{H} + \text{Cl}^-$ collisions (Fig. 4) is similar, except that the dissociation limit of the anion is higher, the highest accessible vibrational level is $\nu = 2$, and the steps due to closing of higher channels can be found both in the $\nu = 0$ and $\nu = 1$ channels. The experiment clearly confirms both of these steps.

The physics underlying the steps S_ν has been discussed by Čížek *et al.* [1] and by Gauyacq [11]. The coupling of the HCl^- or HBr^- resonance to the continuum is very strong, so that the electron is detached with a nearly unity probability as soon as the anion and neutral molecule curves cross. The crossing occurs at a relatively large internuclear distance R , favoring the formation of the product molecule in the highest possible vibrational state, which is $\nu = 1$ for HBr and $\nu = 2$ for HCl for the low collision energies considered here. The spectra thus have steps, labeled $\nu = 0$ and $\nu = 1$ in Figs. 1, 3, and 4, corresponding to the respective rotational onsets $J \geq 0$. The energies of these steps are equal to the center-of-mass collision energy E_{rel} less the energy of the final ($\nu, J = 0$) state; that is, their position shifts to higher ε with increasing collision energy.

When the products HCl or HBr are formed in higher rotational states J (that is, classically speaking, when the impact parameter b of the collision increases), then the energy ε of the detached electrons decreases. These electrons “fill” the regions of the spectrum between the steps. For each J , most of the molecules are created in the state with the highest possible ν , but as J is increased, this highest ν becomes inaccessible. The vanishing of the cross

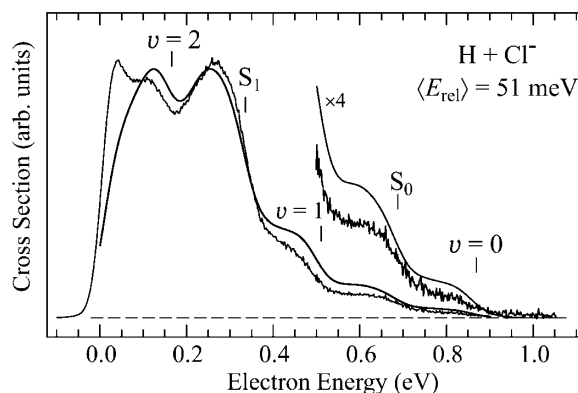


FIG. 4. Experimental and theoretically predicted (smooth curve) spectra of electrons detached in $\text{H} + \text{Cl}^-$ collisions. The laboratory frame ion energy was 0.5 eV.

section for this v is compensated by an increase of the probability for the remaining vibrational states, giving rise to upward (with increasing J ; that is, decreasing ε) steps in the spectrum. The cross sections for the individual rovibrational levels were shown in Ref. [1].

The steps S_v are a manifestation of channel interaction and are closely related to Wigner cusps in dissociative attachment of electrons to hydrogen halides [25], except that here we observe the structures in the J dependence instead of the energy dependence of the cross section. The success of the nonlocal model to reproduce these steps is closely connected to its ability to describe threshold features in low-energy electron scattering in general, including the threshold peaks [26] in vibrational excitation [8,24]. It has long been known [27] that the LCP model ignores the energy dependence of the coupling $V_{d\varepsilon}$, which becomes especially important when the coupling vanishes at opening/closing of channels. The effect is more pronounced if the coupling has a dipole-modified s -wave threshold behavior as in our case. The consequence of this neglect of the energy dependence of $V_{d\varepsilon}$ is a violation of the unitarity of the S matrix in the presence of closing channels [7,28].

In conclusion, the present work demonstrates the necessity of including the interchannel coupling in the calculation of low-energy AD collisions. It has a profound effect on the distribution of the rovibrational states of the product and consequently on the spectrum of the detached electrons. It is quantitatively accounted for by the nonlocal resonance theory. In additional experiments, we have studied the electron spectra at increased collision energies. As expected, the rovibrational onsets are shifted towards higher electron energies with rising collision energy; in contrast, the nonlocal steps S_v remain essentially unshifted, as predicted by the nonlocal resonance theory. These results and a more complete analysis will be reported in a future publication.

We thank I. Bray for providing theoretical cross sections for the excitation of atomic hydrogen and W. Domcke for valuable comments on the manuscript. M.A. and S.Ž. acknowledge support by the Swiss National Science Foundation (Project No. 2000-061543.00), M.Č. and J.H. support by the Grant Agency of the Czech Republic (Projects No. GACR-203/00/1025 and No. GACR-203/00/

D111), F.A.U.T. and H.H. support by the Deutsche Forschungsgemeinschaft through Forschergruppe Niederenergetische Elektronenstreuprozesse.

-
- [1] M. Čížek *et al.*, J. Phys. B **34**, 983 (2001).
 - [2] J.N. Bardsley, A. Herzenberg, and F. Mandl, Proc. Phys. Soc. London **89**, 321 (1966).
 - [3] A. Merz *et al.*, J. Phys. B **27**, 4973 (1994).
 - [4] M. Movre and W. Meyer, J. Chem. Phys. **106**, 7139 (1997).
 - [5] M. Čížek, J. Horáček, and W. Domcke, J. Phys. B **31**, 2571 (1998).
 - [6] F. Fiquet-Fayard, J. Phys. B **7**, 810 (1974).
 - [7] W. Domcke, Phys. Rep. **208**, 97 (1991).
 - [8] M. Čížek *et al.*, Phys. Rev. A **63**, 062710 (2001).
 - [9] B.I. Schneider, M. LeDourneuf, and P.G. Burke, J. Phys. B **12**, L365 (1979).
 - [10] A. Schramm *et al.*, J. Phys. B **32**, 2153 (1999).
 - [11] J.P. Gauyacq, J. Phys. B **15**, 2721 (1982).
 - [12] C.J. Howard, F.C. Fehsenfeld, and M. McFarland, J. Chem. Phys. **60**, 5086 (1974).
 - [13] M.A. Huels *et al.*, Phys. Rev. A **49**, 255 (1994).
 - [14] T.S. Zwier *et al.*, Phys. Rev. Lett. **44**, 1050 (1980).
 - [15] M.A. Smith and S.R. Leone, J. Chem. Phys. **78**, 1325 (1983).
 - [16] M. Allan, J. Electron Spectrosc. Relat. Phenom. **48**, 219 (1989).
 - [17] K.R. Asmis and M. Allan, J. Phys. B **30**, 1961 (1997).
 - [18] A. Stamatović and G.J. Schulz, Rev. Sci. Instrum. **39**, 1752 (1968).
 - [19] M. Allan, Chimia **36**, 457 (1982).
 - [20] F.H. Read and N. Bowring, CPO programming, <http://cpo.ph.man.ac.uk>.
 - [21] B.P. Paolini and M.A. Khakoo, Rev. Sci. Instrum. **69**, 3132 (1998).
 - [22] D. Spence and M. Inokuti, J. Quant. Spectrosc. Radiat. Transf. **14**, 953 (1974); P.D. Burrow (private communication).
 - [23] I. Bray (private communication).
 - [24] M. Čížek, J. Horáček, and W. Domcke, Phys. Rev. A **60**, 2873 (1999).
 - [25] R. Abouaf and D. Teillet-Billy, J. Phys. B **10**, 2261 (1977).
 - [26] K. Rohr and F. Linder, J. Phys. B **8**, L200 (1975).
 - [27] J.N. Bardsley, J. Phys. B **1**, 349 (1968); **1**, 365 (1968).
 - [28] R.J. Bieniek, J. Phys. B **13**, 4405 (1980).